

# The Deformation Effect on the Electronic Structure of the Graphite Nanoribbon Arrays

W . S . Su<sup>1</sup>, B . R . Wu<sup>2</sup> and T . C . Leung<sup>1</sup>

<sup>1</sup>Department of Physics, National Chung Cheng University, Chia-Yi 621, Taiwan

<sup>2</sup>Center for General Education, Chang Gung University, Tao-Yuan 333, Taiwan

(Dated: February 20, 2024)

## Abstract

We have performed a first-principles study on the deformation effect of the electronic structures of graphite nanoribbon arrays with zigzag edges on both sides, and the edge atoms are terminated with hydrogen atoms. A uniaxial strain is considered to have deformation effect on the graphite nanoribbons. We found that the antiferromagnetic arrangement of the spin polarizing edges of graphite nanoribbon is still more favorable than that with the ferromagnetic arrangement under deformation. We also learned that a tensile strain increases the magnetization of the graphite ribbon while a compressive strain decreases it. A positive pressure derivative of the band gap of antiferromagnetic state is observed for the graphite nanoribbon under uniaxial strains. The strain changes the shape of band structure and the band gap; in here, the edge atoms play a crucial role. The deformations are also found to influence the contribution of the edge atoms to the bands near the Fermi level. The deformation effect for the graphite nanoribbon under transverse electric field is also studied.

PACS numbers: 73.22.-f, 81.40.Rs, 75.70.Ak

## I. INTRODUCTION

Since graphene had been successfully synthesized in laboratory [1, 2, 3, 4, 5], graphene and related structures (e.g. carbon nanotubes), ignites intense investigation [6, 7, 8, 9, 10, 11]. That is motivated by the fundamental physics interests and the potentials of versatile applications of the novel structures formed by graphene. A quasi-one-dimensional graphite nanoribbon can be constructed by cutting or by patterning a graphene sheet along a specific direction [4, 5], and it is essentially a strip of graphene with finite width in nanometer size. Owing to the structure being similar to carbon nanotubes, the graphite nanoribbons are expected to have various unique properties and capabilities for the applications of nanoelectronics and nanomechanical devices [5, 8, 9, 10, 11, 12, 13, 14, 15, 16, 17, 18, 19].

The zigzag graphite nanoribbon (ZGNR) is a graphite nanoribbon with zigzag shaped edges. The ZGNRs have the unusual electronic localized edge states, which decay exponentially into the center of the ribbon [6]. The edge states are a twofold degenerate flat band at Fermi level and the flat band is lasting about one-third Brillouin zone (BZ) starting from the zone boundary. While counting the spin polarization effect, the spin states are more favored than the spinless (NM) state. There are two favored spin states: the ferromagnetic (FM) state and the antiferromagnetic (AF) state. The AF (FM) state is the configuration with opposite (same) spin orientation between the two ferromagnetically ordered edges. The ground state of a ZGNR reveals antiferromagnetic. That is, the two edges of the ribbon prefer to exhibit opposite spin orientations and the total spin is zero. Owing to the symmetry breaking and the magnetic interaction between the two edges of a ZGNR [19], the degenerated edge states split into two states with opposite spins and open a gap. The ZGNRs become semiconducting but not metallic [12, 16, 17, 18, 19, 20, 21]. The band gap and the magnetization of edge atoms vary with the width of the ZGNR [12, 19, 21]. The ZGNRs may turn to half-metallic when applied an external electric field across the ribbon that was suggested by Son et al [16]. The effect of external electric field makes the band gap closing in one spin direction and opening in the other spin direction. Following the previous usage, the gap-opening state referred as  $\uparrow$ -spin, and the gap-narrowing state referred as  $\downarrow$ -spin. Besides, the distortions and defects of graphite nanoribbons are also predicted

to have an effect on band structures [15, 22, 23, 24]. In this study, we mainly present the electronic structures of graphite nanoribbons in the presence of a uniform uniaxial strain and a transverse electric field.

## II. CALCULATION METHODS

We consider the deformations of graphite nanoribbons with zigzag edges on both sides and each of the edge atoms passivated by hydrogen atoms on each side. The structure is shown in Fig. 1 (a), and the coordinate axes are defined in Fig. 1 (b). The graphite nanoribbon arrays consist of nanographitic strips that are infinitely long in the  $y$  direction with the primitive cells  $2.441\text{\AA}$  for the ZGNRs. This length is the theoretical result of graphene calculated by density functional theory (DFT) [25] and local density approximation [26]. Several inter-ribbon distances ( $D_x = 3.5$  to  $3.5\text{\AA}$ ) are considered to investigate the inter-layer interaction of the graphite nanoribbon array. The electric field is applied in the  $z$  direction, and the supercell has a vacuum thickness of  $26\text{\AA}$  in the  $z$  direction. A ZGNR is specified by the number of zigzag chains ( $N$ ) along the ribbon forming the width and denote as  $N$ -ZGNR, for example, the structure of Fig. 1 (a) is referred as a 6-ZGNR. As shown in Fig. 1 (a), the width of a ZGNR we defined, here, is the width without including the hydrogen atoms at the edges. The uniaxial stress is imposed in the  $y$  direction, and strain ( $\epsilon$ ) is defined as  $\epsilon = \frac{L - L_0}{L_0}$ .

This work is performed within the DFT and the local spin density approximation (LSDA) via the Vienna ab initio simulation package (VASP) [27, 28, 29]. The exchange-correlation energy is in the Ceperley-Alder form [30] and the ultrasoft pseudopotentials [28] are used. The plane-wave cutoff up to  $358.2\text{ eV}$  has been carried out and the  $1 \times 80 \times 1$   $k$ -points sampling in the first BZ is used. The atomic positions are relaxed until the magnitudes of the forces become less than  $0.01\text{ eV/\AA}$ , and the total energies are converged to within  $1\text{ meV}$ . In order to simulate a homogenous external electric field ( $F$ ) in the  $z$ -direction (Fig. 1), a dipole sheet ( $xy$ -plane) perpendicular to the ribbon edge is placed at the center of the vacuum region in the supercell. A dipole correction is included to avoid artificial Coulomb interactions caused by the external electric field.

### III. RESULTS AND DISCUSSIONS

The deformation effect on the ZGNRs with various widths is studied by giving a uniaxial strain along the y-direction. For the undeformed ZGNRs, we also got that the AF state is the ground state, and the total energy of the AF state is lower than that of the FM (NM) state with few (tens) meV per edge atom. The total energy difference  $E_{FM-AF}$  ( $E_{NM-AF}$ ) between the AF and FM (NM) states of a ZGNR lowers (raises) as the undeformed ZGNR gets wider, it agrees with the results of the previous studies [12]. For the deformed ZGNRs, the AF state remains the ground state and the NM state is still less favored than the spin states. The trend of the  $E_{NM-AF}$  and  $E_{FM-AF}$  varying with the widths of the ZGNRs is still retained as the ZGNRs are under the same strain. Fig. 2 (a) gives the variations of the

$E_{FM-AF}$  under various strains. The  $E_{FM-AF}$  raises as the strain increases. It reveals that the AF state becomes more stable than the FM state for the ZGNR under a tensile strain. However, the deformation effect on the  $E_{FM-AF}$  of a ZGNR is less significant when the ZGNR gets wider. Since the AF state is the ground state of the ZGNRs under strains, here, we only discuss the deformation effect on the AF spin state. As can be seen in Fig. 2 (b), the magnetization of a ZGNR increases as the strain gets large and the ribbon gets wider. It indicates that the magnetic interaction between the edge atoms of both sides of ribbon increases under tensile strains, while it decreases as the ZGRN gets wider. As a result, the increasing (decreasing) of the magnetic interaction raises (lowers) the  $E_{FM-AF}$  of ZGNRs.

Figs. 3 (a) and 3 (b) are corresponding to the variation of band gap of undeformed ZGNRs and magnetic moment with the width ( $w$ ), and the band structures are given in Fig. 3 (c). The band gap increases firstly and then decreases as inversely proportional to the width of N-ZGNR for  $N \geq 8$  [12]. As the magnetic interaction of the two edges of the ribbon is one of the reasons to create the band gap of the degenerate edge states, the strength of the magnetization is related to the variation of the band gap [19]. The magnetic interaction is proportional to the square of the magnetization, while the interaction energy is also inversely proportional to the width of a ZGNR. Therefore, the band gap of the AF state of a ZGNR shall be proportional to the square of the magnetization and the inverse of the width of a ZGNR. The magnetization of the spin state raises exponentially and saturates when the

width of ribbon is greater than 15Å [Fig.3 (b)]. As a result, the variation of the band gap seems be dominated by the width of ZGNR as the width of ribbon is greater than 15Å [12]. Though the electron spin density of a ZGNR is mostly localized around the edge atom, the magnetic interactions of other atoms near the ribbon edge are not negligible, especially for a short ZGNR ( $w < 15\text{Å}$ ). While counting the contributions of the edge atoms and other atoms near the ribbon edges to the magnetic interaction, the calculated band gap can be fitted to the eq. (1) below:

$$E_g = 479.07 \frac{m_1^2}{w + 36.80} + 913.11 \frac{m_2^2}{w - 1.81} \quad (1)$$

Where  $m_1$  and  $m_2$  are corresponding to the magnetic moments of edge atom, and other atoms near the ribbon edge, and  $w$  is in Å. Similar to the ribbon without deformation, the band gap of a wide ZGNR under a fixed strain also shows inversely proportional to the width of the ZGNR. As shown in Fig.3 (c), the ZGNRs have flat conduction edge band and the slope of the valence edge band shows no significant change except for 2-ZGNR. The magnetic interaction takes the conduction and valence edge bands apart and makes little change in the shape of the edge bands except for that of 2-ZGNR.

Fig. 4 (a) gives the band gaps of the AF states with various strains. We find a positive pressure derivative of band gap of ZGNRs. The band gap of a ZGNR under uniaxial strains shows an interesting behavior. The band gap of a ZGNR gets opening under compressive strains ( $\epsilon < 0$ ), and reaches a maximum at a critical compressive strain  $\epsilon_c$ ; then turns to get closing as the ZGNR is continuously compressed. On the contrary, the band gap of a ZGNR gets closing under tensile strains ( $\epsilon > 0$ ). The band gap of a ZGNR becomes continuously opening and reaches to a minimum at a critical tensile strain  $\epsilon_T$ , then gets opening while the ribbon is continuously elongated. As can be seen in Fig. 4 (a), the critical compressive (tensile) strain  $\epsilon_c$  ( $\epsilon_T$ ) are related to the width of a ZGNR,  $\epsilon_c$  decreases and  $\epsilon_T$  increase, as the ribbon gets wider. The strain induced band gap variation of a wide ribbon is stronger than that of a narrow one. In Fig. 4 (b), the edge bands of 10-ZGNR under strains are plotted. We found that band structure of a ZGNR is sensitive to the strain. It is notable the uniaxial strain changes the shape of the band structure of a ZGNR, especially the conduction edge band. The band bending of the edge states dominates the behavior of band gap of the deformed ZGNR. In addition to the factor of band bending, the magnetic

interaction is the other factor to affect the behavior of band gap. For an elongated ZGNR, the band bending tends to open the band gap, while the magnetic interaction to close. The competition of the two factors determined the behavior of the band gap of a ZGNR under strains.

For a deformed ZGNR, a tensile strain increases the magnetization of the edge atoms [Fig. 2 (b)] but decreases the width of the ribbon; while a compressive strain gives oppositely results. Following the rule of the magnetic interaction to the band gap of a ZGNR state above, a ZGNR shall have a negative pressure coefficient of band gap. However, the band gap of a ZGNR has a positive coefficient rather than a negative one for  $\epsilon_c < \epsilon < \epsilon_T$ ; whereas, it has a negative pressure coefficient for  $\epsilon < \epsilon_c$  and  $\epsilon_T < \epsilon$ . As can be seen in Fig. 4 (b), the gap of the edge states at  $k_F$  (Here, the wave vector of the top of the valence band is referred as  $k_F$ ) and BZ boundary gets apart under a tensile strain, while the gap gets closing under a compressive strain. Thus, a stronger magnetic interaction corresponds to a larger gap. It reveals the magnetic interaction actually affects the edge bands of ZGNRs under strains. When strain is in the region of  $\epsilon_c < \epsilon < \epsilon_T$ , a ZGNR has a positive pressure derivative of band gaps. Similarly, the band gap of diamond also exhibits a positive pressure derivative. However, the mechanism of both cases is different. The opening of the band gap of diamond is due to the apart of conduction and valence bands, while the variation of band gaps of ZGNR is caused by band bending of the conduction edge band. Strain makes the edge bands bending and the band bending of conduction edge band determines the variation of band gap. Compressive strains lowered the conduction edge band near  $k_F$  point and lifted the conduction edge band near the BZ boundary. The minimum of the conduction edge band is at the BZ boundary as  $\epsilon > \epsilon_c$ , while shift to  $k_F$  at the critical compressive strain of  $\epsilon_c$ . For a ZGNR under a compressive strain, the minimum of conduction edge band is lifted and causes the gap opening. As strain is in the region of  $\epsilon < \epsilon_c$  or  $\epsilon > \epsilon_T$ , the effect of magnetic interaction exceeds that of band bending. Thus, the band gap of a ZGNR reaches a maximum at the critical compressive strain ( $\epsilon_c$ ).

As shown in Fig. 4 (b), the edge bands of an undeformed 10-ZGNR is lasting around one-fourth BZ starting from the BZ boundary, and the top of the valence band locates at  $k_F = 0.75 \pi/a_y$ . As the strain increases, the  $k_F$  shifts to low wave vector and the edge bands

extend to the low  $k$  region. Moreover, the edge band extends more than one-third of BZ as the strain is up to 0.12. The edge bands of the ZGNR under a tensile strain are longer and steeper than the ZGNR under a compressive strain. It is found that tensile strain reduces the contribution of the edge atoms to the edge bands near the BZ boundary but raises that for  $k_F < k < 0.9\pi/a_y$ . It is contrary while ZGNRs is under compressive strains. As for the edge band of  $\uparrow$ -spin state, the valence edge band is mainly contributed by the edge atoms at one side of the ribbon, while the conduction edge band by the edge atoms at the other side. In the same manner, the edge band of  $\downarrow$ -spin is mainly contributed by the edge atoms at opposite side. When the ribbon is under tensile strains, the edge bands near the BZ boundary are both lowered, while the conduction edge band near  $k_F$  point is lifted. Thus, both the edge bands become steeper when the ribbon is under tensile strains. However, the conduction edge band near the BZ boundary turns to be lifted as  $\epsilon > \epsilon_T$ . As a result, the band gap of the ribbon becomes opening for  $\epsilon > \epsilon_T$ . However, the strain changes the shape of the edge band of the ZGNRs. The variation of band gap is dominated by the band bending of the edge states for  $\epsilon_c < \epsilon < \epsilon_T$ , while dominated by the magnetic interaction for the strain in the region of  $\epsilon < \epsilon_c$  and  $\epsilon > \epsilon_T$ .

With applied transverse electric fields, the band gap of a ZGNR related to  $\uparrow$ -spin get wide, while the band gaps related to  $\downarrow$ -spin get narrow. Similar to the previous study of a ZGNR under external field, the reduction and increasing of the band gap strongly depends on the width of the ZGNR. When applied the same strength of electric field, a wide ZGNR is easier to reach the half-metallic state than the narrow one. That is owing to the reduction of the band gap depends on the voltage between the two edges, and the voltage is proportional to the width of the ZGNR. We also investigate the deformed ZGNR under transverse external electric fields. The variation of band gap of the deformed 10-ZGNR with external electric fields is shown in Fig. 5(a) and the band structures of the undeformed 10-ZGNR with external electric fields are given in Fig. 5(b). With external electric field, the band gaps of deformed ZGNRs are all reduced no matter how the strain is compressive or tensile. When applied a fixed external electric field, the behavior of band gaps of a ZGNR with various strains is similar to that without external electric field. Besides, the value of the critical compressive strain  $\epsilon_c$  increases as the strength of the external field increases, as can be seen in Fig. 5(a). Because the external electric field and the compressive strain both title the

conduction edge band, but in opposite directions [see Fig. 5(b) and Fig. 4(b)]. It needs larger strain to against the effect caused by electric field, as a result, the critical compressive strain increases under a transverse electric field.

#### IV . CONCLUSIONS

Conclusively, we have performed a detailed investigation of the ZGNRs under uniaxial strains and under external transverse electric fields. The antiferromagnetic state of a ZGNR remains the ground state under deformations. A tensile strain increases the magnetization of the ZGNR, while a compressive strain decreases it. An interesting behavior of band gaps of the ZGNRs under strains is found. The strain changes the shape of the band structure and the band bending of conduction edge band dominate the variation of band gap for  $\epsilon_c < \epsilon < \epsilon_T$ . The band gap of the AF state of a deformed ZGNR is also reduced with an external electric field. As the applied an external electric field is fixed, the behavior of the band gap with various strains is similar to that without external electric fields.

#### V . ACKNOWLEDGEMENT

We would like to acknowledge the National Center for Theoretical Sciences (NCTS) in Taiwan and the financial support from National Science Council (NSC) of Taiwan under Grant Nos. NSC 96-2738-M-002-003 and NSC 96-2112-M-194-012-MY3, and from a grant of computer time at the National Center for High Performance Computing in Taiwan.

- 
- [1] K .S.Novoselov, et al, Science 306, 666 (2004).
  - [2] Y .Zhang, Y .W .Tan, H .L.Stormer, and P .K in , Nature (London) 438, 201 (2005).
  - [3] K .S.Novoselov et al, Nature (London) 438, 197 (2005).
  - [4] S.Stankovich et al, Nature (London) 442, 282 (2006).
  - [5] C .Berger et al, Science 312, 1191 (2006).
  - [6] M .Fujita, K .W akabayashi, K .Nakada, and K .Kusakabe, J.Phys.Soc.Jpn. 65, 1920 (1996).
  - [7] K .S.Novoselov et al, Science 315, 1379 (2007).
  - [8] M .I.Katsnelson, M aters. Today 10, 20 (2007).



- [9] S.F.Huang, T.C.Leung, Bin Li, and C.T.Chan, Phys.Rev.B 72, 035449 (2005).
- [10] C.P.Chang, B.R.Wu, R.B.Chen, and M.F.Lin, J.Appl.Phys. 101, 063506 (2007)
- [11] H.R.Gutierrez, U.J.Kim, J.P.Kim, and P.C.Eklund, Nano Lett. 5, 2195 (2005).
- [12] Y.-W.Son, M.L.Cohen, and S.G.Louie, Phys.Rev.Lett. 97, 216803 (2006).
- [13] K.Wakabayashi, M.Fujita, H.Ajiki, and M.Sigrist, Phys.Rev.B 59, 8271 (1999).
- [14] M.F.Lin and F.L.Shyu, J.Phys.Soc.Jpn. 69, 3529 (2000).
- [15] M.Fujita, M.Igami, and K.Nakada, J.Phys.Soc.Jpn. 66, 1864 (1997).
- [16] Y.-W.Son, M.L.Cohen, and S.G.Louie, Nature 444, 347 (2006).
- [17] V.Barone, O.Hod, and G.E.Scuseria, Nano Lett. 6, 2748 (2006).
- [18] E.Rudberg, P.Sa?ek, and Y.Luo, Nano Lett. 7, 2211 (2007).
- [19] L.Pisani, J.A.Chan, B.Montanari, and N.M.Harrison, Phys.Rev.B 75, 064418 (2007).
- [20] L.Yang, C.H.Park, Y.-W.Son, M.L.Cohen, and S.G.Louie, Phys.Rev.Lett. 99, 186801 (2006).
- [21] M.Y.Han, B.Ozyilmaz, Y.Zhang, and P.Kim, Phys.Rev.Lett. 98, 206805 (2007).
- [22] R.Khare et al., Phys.Rev.B 75, 075412 (2007).
- [23] H.Kajii, K.Yoshino, T.Sato, and T.Yamabe, J.Phys.D 33, 3146 (2000).
- [24] T.Yamabe, M.Imade, M.Tanaka, and T.Sato, Synth.Met. 117, 61 (2001) (2007).
- [25] P.Hohenberg, W.Kohn, Phys Rev 136 B 864 (1964).
- [26] W.Kohn, L.J.Sham, Phys Rev. 140 A 1133 (1965).
- [27] G.Kresse and J.Hafner, Phys.Rev.B 47, R 558 (1993).
- [28] G.Kresse and J.Hafner, J.Phys.: Condens.Matter 6, 8245 (1994).
- [29] G.Kresse and J.Furthmüller, Comput.Mater.Sci. 6, 15 (1996).
- [30] D.M.Ceperley, B.J.Alder, Phys Rev Lett. 45 566 (1980).

## VI. FIGURE CAPTIONS

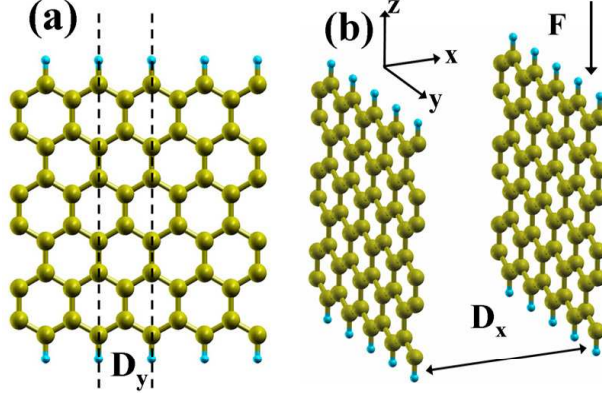


FIG .1: (Color online) (a) Structure of the 6-ZGNR. The boundary of the primitive cell in the y direction is shown with the dashed lines. (b) Orientation of the unit cell for the graphite nanoribbons with edges terminated by H atoms (small blue circles). The external electric field  $F$  is represented by an arrow.

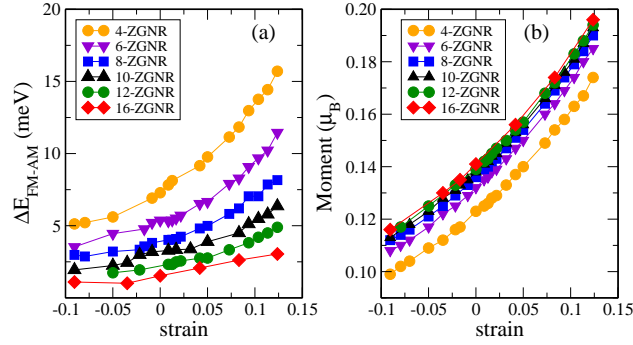


FIG .2: (Color online) (a) Total energy difference between AF state and FM state ( $E_{FM} - E_{AF} = E_{FM} - E_{AF}$ ) as a function of strain with various lengths. (b) Magnetic moment of AF state as a function of strain with various lengths.

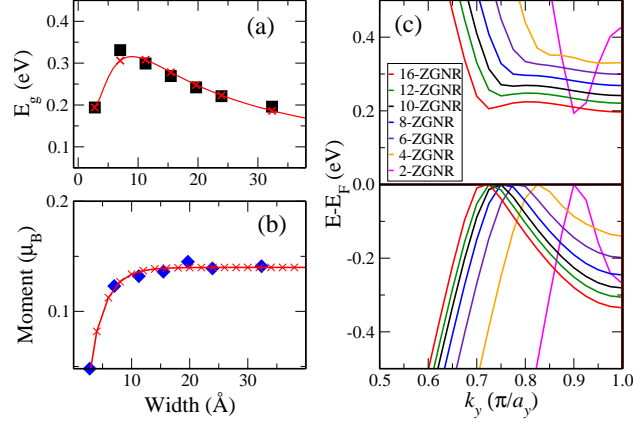


FIG . 3: (Color online) (a) Energy gap as a function of width of ZGNR. (b) Magnetic moment of AF state as a function of width of ribbon. (c) The edge band of the undeformed ZGNRs with various widths.

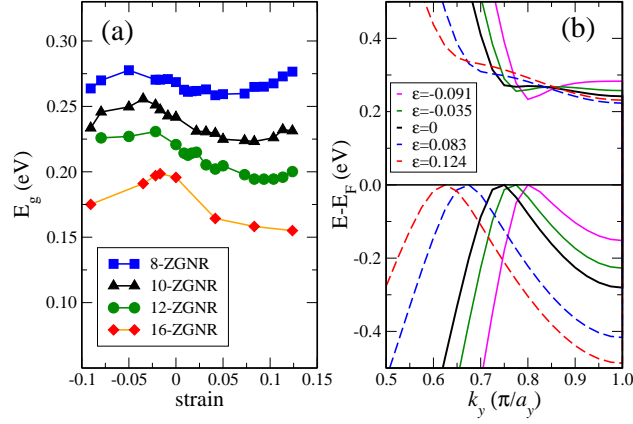


FIG . 4: (Color online) (a) Energy gaps of the ZGNRs as functions of strain with various widths. (b) The edge band of the 10-ZGNR under various strains. Solid lines and dashed lines represent the band structure with compressive and tensile strain, respectively.

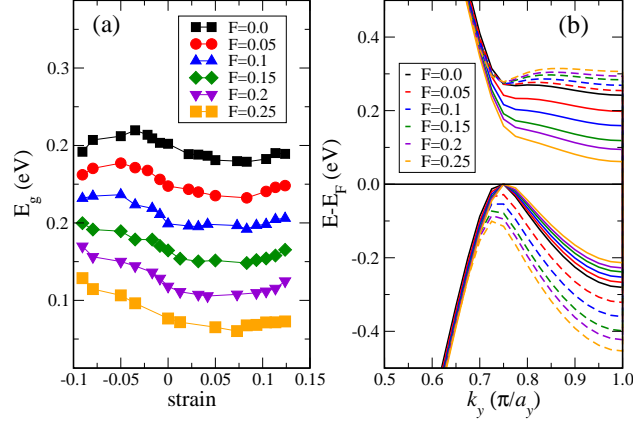


FIG .5: (Color online) (a) The band gaps of the 10-ZGNR with external electric field as a function of strain. (b) The band structure of an undeformed 10-ZGNR under external electric field. The dashed lines and solid lines are shown as  $\downarrow$ - and  $\uparrow$ -spin states. The line of colors in black, red, green, blue, cyan and pink denote the external electric field  $F=0, 0.05, 0.1, 0.15, 0.2$ , and  $0.25$  V/Å, respectively.